USDOT Region V Regional University Transportation Center Final Report

Sensor Network Design for Multimodal Freight Transportation Systems

By

Xiaopeng Li
Ph.D. student
Civil and Environmental Engineering
University of Illinois, Urbana-Champaign
li28@uiuc.edu

and

Eunseok Choi
Undergraduate student
Civil and Environmental Engineering
University of Illinois, Urbana-Champaign
choi22@uiuc.edu

and

Yanfeng Ouyang
Principal Investigator
Assistant Professor of Civil and Environmental Engineering
University of Illinois, Urbana-Champaign
yfouyang@uiuc.edu

DISCLAIMER

USDOT Region V Regional University Transportation Center Final Report

TECHNICAL SUMMARY

Sensor Network Design for Multimodal Freight Transportation Systems

Introduction

The agricultural and manufacturing industries in the US Midwest region rely heavily on the efficiency of freight transportation systems. While the growth of freight movement far outpaces that of the transportation infrastructure, ensuring the efficiency and sustainability of the transportation networks becomes a major challenge. The prominent disbenefit of delay and unreliability highlights the need for an integrated, systems-level framework that incorporates cutting-edge information technologies and advanced multimodal network modeling techniques to monitor, manage and plan complex freight transportation systems. Recent developments in sensing and information technology hold the promise to allow efficient monitoring, assessment, and management of complex systems.

Findings

This project investigated the effect of existing or off-the-shelf sensors on detecting traffic and infrastructure conditions for highway and rail modes. This research project developed an analytical framework to quantify the benefits and costs of deploying sensors for the major freight transportation modes. Specifically, this project developed a new sensor deployment problem in the context of traffic O-D flow surveillance using vehicle ID inspection technologies (e.g., RFID). In addition to traditional flow coverage benefits based on individual sensors, we investigated the path coverage benefits from synthesizing the multiple sensors in transportation networks. We considered possible sensor disruptions that are very common for many sensor technologies, yet not well addressed until very recently.

A reliable location design model framework was proposed to optimize sensor deployment benefit. This model considered both flow and path coverage, while allowing for probabilistic sensor failures. A set of efficient algorithms were developed and tested on moderate-size problem instances. We found that the LR-based algorithm had the best performance for the tested problems. The greedy-algorithm can yield good solutions if flow coverage benefit is significant.

Then we applied this model to the large-scale Chicago intermodal network, where the highway network, the railroad network and their connections were considered in this study. We extracted detailed input flow data from limited data resources. We examined the qualities of solutions of different algorithms, the best of which (from the LR-based algorithm) are analyzed to draw out managerial insights about sensor deployment. The experiments showed that path coverage benefit is more sensitive to sensor failures and installation budget. It was also found that path coverage tends to spread out sensor locations while high failure probabilities tend to cluster sensors together.

Recommendations

Future work can be conducted in several directions. First of all, the proposed model addresses probabilistic sensor failures but assumes known O-D flow paths. This may be reasonable in the freight operation context but a more comprehensive model that encompasses traffic routing and assignment will be desirable. In addition, the current model assumes all sensor failures are independent with equal probability. Yet more complex sensor failure patterns (e.g, site-dependent and correlated failures) are not uncommon in the real world. Additional work that relaxes these two assumptions is needed. Finally, it will be interesting to explore how alternative traffic surveillance benefits would affect the optimal sensor deployment pattern.

Contacts

For more information:

Yanfeng Ouyang
Principal Investigator
Civil and Environmental Engineering
University of Illinois, Urbana-Champaign
yfouyang@uiuc.edu
(217) 333-9858
(217) 333-1924 Fax

NEXTRANS Center
Purdue University - Discovery Park
2700 Kent B-100
West Lafayette, IN 47906

nextrans@purdue.edu
(765) 496-9729
(765) 807-3123 Fax

www.purdue.edu/dp/nextrans

USDOT Region V Regional University Transportation Center Final Report

Sensor Network Design for Multimodal Freight Transportation Systems

By

Xiaopeng Li
Ph.D. student
Civil and Environmental Engineering
University of Illinois, Urbana-Champaign
li28@uiuc.edu

and

Eunseok Choi
Undergraduate student
Civil and Environmental Engineering
University of Illinois, Urbana-Champaign
choi22@uiuc.edu

and

Yanfeng Ouyang
Principal Investigator
Assistant Professor of Civil and Environmental Engineering
University of Illinois, Urbana-Champaign
yfouyang@uiuc.edu

Report Submission Date: October 15, 2009

ACKNOWLEDGMENTS

TABLE OF CONTENTS

LIST OF FIGURES

CHAPTER 1. INTRODUCTION

1.1   *Background and motivation*

The US Midwest region generates about 20 percent of the nation's overall gross domestic product (GDP). The backbone industries (such as agriculture and manufacturing) and regional economy are heavily dependent of the efficiency of regional freight transportation systems. While the transportation infrastructure development has reached a plateau in recent years (approximately one percent increase of lane miles per year) 1, the volume of freight movement has been growing, and will continue to grow, dramatically. It is estimated that the number of freight trucks in the Midwest states will increase by more than 60 percent by 2020 (Meiller 2007). As the demand for freight transportation infrastructure continues to grow at an increasing pace, ensuring the efficiency and sustainability of the transportation networks for current and future generations is a major challenge. Nationwide, after 40 years of steady declination, freight logistics costs have been rising again in both absolute quantity and percentage GDP. A significant portion of this cost increase has been attributed to the deterioration of delay and unreliability in our highly congested freight transportation systems across modes (highway, rail, ocean waterway). This poses prominent disbenefits to the society and highlights the need for an integrated, systems-level framework that incorporates cutting-edge information technologies and advanced multimodal network modeling techniques to monitor and manage the complex freight transportation systems. Such an integrated framework will enable decision makers to (1) understand conditions of multiple system components (traffic, infrastructure, etc.) at various spatial and temporal scales, and (2)

identify effective planning and management solutions to achieve desirable operating conditions and ensure efficient operations of freight transportation across modes.

Recent developments in sensing and information technology and its applications to the field of transportation hold the promise to allow efficient monitoring, assessment, management, and planning of complex networks with system-wide interactions among multiple system components. This is possible by combining information from parallel sensing systems with integrated multi-scale modeling and decision support. State transportation agencies have made significant investment in deploying various types of sensors (e.g., loop detectors, RFID transponders) on state and local highways, which enable a wide range of fundamental applications in traffic management systems (TMS) such as traffic condition surveillance (e.g., incident detection), prediction (e.g., travel time estimation), and control (e.g., freeway ramp metering and traffic diversion). Prior success on traffic database development and travel time prediction have demonstrated the benefit of collecting traffic and speed data from loop detectors, radar sensor stations, and toll collection transponders. The railroads have also invested millions of dollars in advanced sensing technology (e.g., track-side machine vision devices) to monitor railcar traffic.

1.2 *Literature review and study objectives*

Sensor technologies (e.g., loop detectors, surveillance cameras, radio frequency identifications/RFID) have been widely used on transportation networks. Real-time traffic information is sampled by these sensors to monitor traffic status and to develop control strategies. The effectiveness of a traffic surveillance system depends on not only the accuracy of the sampled information but also the coverage over the transportation network. However, implementing these new technologies usually requires large investment. Accuracy and coverage are often two conflicting objectives due to limited resources: collecting high-quality information usually relies on sophisticated and expensive technologies and thus limited budget would restrict the number of installations; on the other hand, due to the limited effective range of most sensors, complete coverage

over a network usually requires dense installations. To balance this trade-off, intensive studies have been conducted to determine efficient and reliable deployment of surveillance systems. Yang et al. (1991) conducted a robust analysis on the utility of traffic counting points for traffic O-D flow estimation. Yang and Zhou (1998) proposed a sensor deployment framework to maximize such utility. This framework has been extended to accommodate turning traffic information (Bianco et al., 2001), existing installations and O-D information content (Ehlert et al., 2006), screen line problem (Yang et al., 2006), time-varying network flows (Fei et al., 2007; Fei and Mahmassani, 2008) and railcar inspection under potential sensor failures (Ouyang et al., 2009).

Despite numerous studies on O-D flow coverage, research on the usage of sensors for network O-D travel time estimation has been relatively scarce. To the best of our knowledge, only Banet al. (2009) developed sensor deployment algorithm for travel time estimation in a single freeway corridor---little research has addressed the problem in general networks. Accurate travel time estimation provides important information for decision support in both private sectors (e.g., tacking fleets for trucking companies, traveler information provision) and public agencies (e.g., congestion mitigation, accident management). For a transportation network, we may want to know as much as possible the real-time travel time between all possible O-D pairs. However, traditional surveillance technologies (e.g., loop detectors) would encounter significant challenges due to their inability to accurately capture O-D flows (Kerner and Rehborn, 1996; Li et al., 2009). New sensor technologies, on the other hand, are able to identify vehicle IDs and therefore hold the promise to overcome these challenges by synthesizing vehicle ID information from different sensors. For example, the consecutive time stamps of a vehicle at two sensor locations would provide an accurate estimate of travel time.

Despite numerous studies on O-D flow coverage, research on the usage of sensors for network O-D travel time estimation has been relatively scarce. To the best of our knowledge, only Ban et al. (2009) developed sensor deployment algorithm for travel time estimation in a single freeway corridor---little research has addressed the problem in general networks. Accurate travel time estimation provides important information for decision support in both private sectors (e.g., tacking fleets for trucking companies,

traveler information provision) and public agencies (e.g., congestion mitigation, accident management). For a transportation network, we may want to know as much as possible the real-time travel time between all possible O-D pairs. However, traditional surveillance technologies (e.g., loop detectors) would encounter significant challenges due to their inability to accurately capture O-D flows (Kerner and Rehborn, 1996; Li et al., 2009). New sensor technologies, on the other hand, are able to identify vehicle IDs and therefore hold the promise to overcome these challenges by synthesizing vehicle ID information from different sensors. For example, the consecutive time stamps of a vehicle at two sensor locations would provide an accurate estimate of travel time.

Like many other IT technologies, most existing sensors are subject to performance disruptions due to system errors, adverse weather conditions, or intentional sabotages (Rajagopal and Varaiya, 2007; Carbunar et al., 2005). Intuitively, such failures may substantially impair the surveillance effectiveness. Potential disruptions need to be addressed in a reliable design so that the sensor system not only has a good performance in the normal scenario but also is resilient against possible loss in failure scenarios. In recent years, reliable facility location problems have been studied in the supply chain design (Daskin, 1983; Snyder and Daskin, 2005; Cui et al., 2009; Li and Ouyang, 2009) and railroad defect detection sensor design contexts (Ouyang et al., 2009). However, despite these recent efforts, few studies in the network traffic surveillance context have addressed the possibility of sensor failures.

This research aims to fill these gaps. It builds on the reliable facility location literature and develops a linear integer model to determine optimal locations for vehicle ID inspection sensors for travel time estimation as well as traffic O-D flow count. The model allows probabilistic sensor failures in general transportation networks. The formulated problem is complex by nature, and the real-world instances are generally of large scale. This imposes prohibitive computational burden if we solve this model with standard solvers. We therefore propose customized algorithms to solve the problem efficiently. Case studies are conducted to test the algorithms and to draw insights.

1.3   *Organization of the research*

The remainder of the research is organized as follows. Chapter 2 develops the mathematical model and proposes different algorithms to solve this problem. The performance of these algorithms is tested with a moderate-size example. We found the Lagrangian-relaxation-based algorithm outperforms the others in general. Chapter 3 applies this model to a large-scale real problem, the Chicago intermodal network. A set of data-processing procedures including heuristics have been taken to extract detailed input from limited macroscopic data. Managerial insights are drawn from result analysis. Chapter 5 summarizes the research and provides future research directions.

CHAPTER 2. MODELING AND SOLUTION TECHNIQUES

This chapter introduces the model formulation and solution algorithms. Section 2.1 formulates the problem into a mathematical model. Section 2.2 introduces solution algorithms and analyzes their properties. Section 2.3 tests these algorithms with a moderate-scale example and discusses their performances.

2.1   *Model introduction*

Flow Coverage

Path Coverage
(length dependent)
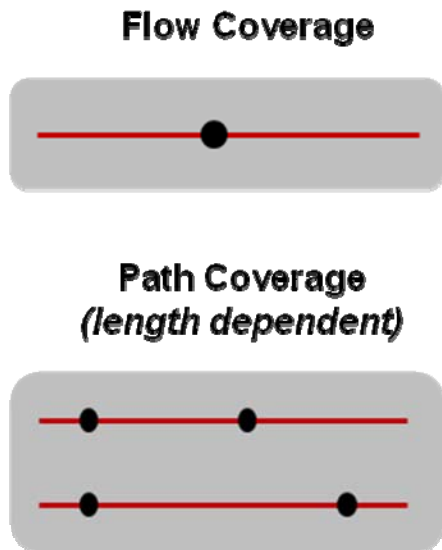
Fig. 2 Flow and Path Coverage

We select sensor locations in a transportation network to maximize the expected benefit from both O-D volume estimation and travel time measurement. For any O-D flow, the total traffic volume can be inspected by a single sensor if and only if the flow passes the sensor (Yang and Zhou, 1998). In this case, we say that the flow is covered by the sensor in the sense of flow coverage (see figure 2). Such individual sensor information can also be used to infer travel time based on speed measurements (Ban et al., 2009). However, sensors (particularly those with vehicle-ID capabilities; e.g., RFID) can work in pairs to provide an accurate measurement of travel time between their installation locations. Assume that the traffic state along the traffic paths remains

relatively stable during the nominal travel time. 1 Intuitively, accurate travel time estimation for an O-D path benefits all traffic on this path, while the accuracy depends on the span of sensors---the wider a pair of sensors span over an O-D path, the larger portion of the path is measured and the better it helps to estimate travel time of that O-D path. Thus the travel time surveillance benefit, which we denote by path coverage (see figure 2), depends on not only the inspected traffic volume but also the lengths of covered O-D paths by sensor pairs. We assume for simplicity that path coverage for an O-D path is proportional to both its traffic volume and covered length.

Let $\mathcal{I}$ be the set of O-D paths on the network. Each path $i \in \mathcal{I}$ is specified by its traffic volume f_i, which is assumed to be deterministic and known. Each path i passes a set of candidate locations, $\mathcal{J}_i$, where sensors can be potentially installed. Each candidate location j on path i has a corresponding mileage, m_{ij}, increasing along the traffic direction of f_i. The collection of all candidate locations over the network is $\mathcal{J} := \bigcup_{\forall i} \mathcal{J}_i$. For convenience of notation, let $\mathcal{I}_j$ denote the set of paths that pass the same location j. Note that $\bigcup_{\forall j} \mathcal{I}_j = \mathcal{I}$.

Due to limited budget, no more than N sensors can be built on the network. For $\forall i \in \mathcal{I}_j$, f_i is inspected if an operational sensor is located at j. Similar to the traditional maximal covering models (Yang and Zhou, 1998), if f_i is inspected by at least one sensor, the benefit of flow coverage is $b_c f_i$, where b_c is a nonnegative coefficient. If f_i passes at least two sensors, we can record its travel time between the first functioning (*head*) sensor it passes, at location j^h, and the last functioning (*rear*) sensor it passes, at location j^e. The benefit of path coverage can be expressed as $b_t f_i (m_{ij^e} - m_{ij^h})$, where b_t is also a nonnegative coefficient.

---

[1] Without losing generality a path can be divided into multiple short segments to make this assumption reasonable.

In the long run, sensors may be disrupted or malfunctional from time to time. When sensors fail, the flow coverage and path coverage patterns in the network also change. Hence we consider the expected surveillance benefit across all sensor failure scenarios in addition to the ideal non-failure scenario. The head (or rear) sensor for each i may vary over different failure scenarios. In other words, different head (or rear) sensors are assigned to i according to failure scenarios. Sensors on i can be ranked into different priority levels according to such head (or rear) assignment such that in any scenario the sensor with the lowest level among all functioning ones, if available, is the head (or rear) sensor. In the normal scenario (without any failure), the most upstream sensor on i serves as the head sensor, and thus it is the level-zero head sensor for i. If this sensor fails, its immediately downstream sensor takes over to serve i, and thus this second sensor is the level-one head sensor for i. This process can be repeated to label every installed sensor on i with a unique head sensor assignment level. Similarly, each sensor on i can be labeled with a unique rear sensor assignment level that starts from zero for the most downstream sensor and increases upstream. Supposing that there are S_i sensors installed on path i, we see that once the locations with installations on i are given (i.e., $\{j_0^i, j_1^i, .., j_{S_i-1}^i\}$ ordered from upstream to downstream), their head and rear assignment levels are determined by the following simple rule

Definition 1. (*valid assignment rule*) A sensor at location j_s^i is the level-s head sensor and the level-$(S_i - 1 - s)$ rear sensor for traffic path i.

Since each sensor installed on i receives a unique head (or rear) assignment level to i, there are at most $R_i := \min(|\mathcal{J}_i|, N)$, levels of possible head (or rear) assignment. Let $r = 0, 1, \cdots, R_i - 1$ denote a possible head (or rear) assignment level for a sensor on i.

The primal decision variables $\mathbf{x} := \{x_j\}$ determine where to install sensors, where

$$x_j = \begin{cases} 1, & \text{if a sensor is installed at location } j; \\ 0, & \text{otherwise.} \end{cases}$$

Given $\mathbf{x}$, the auxiliary variables $\mathbf{h} = \{h_{ijr}\}$ and $\mathbf{e} = \{h_{ijr}\}$ decide how sensors are assigned to paths according to the valid assignment rule; i.e.,

$$h_{ijr} = \begin{cases} 1, & \text{if a sensor is installed at } j \text{ and it is assigned to } i \text{ as a level-}r \text{ head sensor;} \\ 0, & \text{otherwise,} \end{cases}$$

and

$$e_{ijr} = \begin{cases} 1, & \text{if a sensor is installed at } j \text{ and it is assigned to } i \text{ as a level-}r \text{ rear sensor;} \\ 0, & \text{otherwise.} \end{cases}$$

Assume that each sensor fails independently with an identical probability $0 \le q < 1$. The objective of this two-sensor-covering problem (TSC) is to maximize the expected total benefit of flow coverage and path coverage for all O-D paths.

$$(\text{TSC}) \quad \max_{\mathbf{x}} z(\mathbf{x}) := \max_{\mathbf{h},\mathbf{e}} \sum_{i \in \mathcal{I}} \sum_{j \in \mathcal{J}_i} \sum_{r=0}^{R_i - 1} q^r (1-q) f_i [-b_t m_{ij} h_{ijr} + (b_t m_{ij} + b_c) e_{ijr}], \quad (1)$$

$$\text{subject to} \qquad \sum_{j \in \mathcal{J}} x_j \le N, \tag{2}$$

$$\sum_{r=0}^{R_i - 1} h_{ijr} = x_j, \forall i \in \mathcal{I}, \forall j \in \mathcal{J}_i, \tag{3}$$

$$\sum_{r=0}^{R_i - 1} e_{ijr} = x_j, \forall i \in \mathcal{I}, \forall j \in \mathcal{J}_i, \tag{4}$$

$$\sum_{j \in \mathcal{J}_i} h_{ijr} \le 1, \forall i \in \mathcal{I}, r = 0; \tag{5a}$$

$$\sum_{j \in \mathcal{J}_i} h_{ijr} \le \sum_{j \in \mathcal{J}_i} h_{ij(r-1)}, \forall i \in \mathcal{I}, \forall r = 1, \cdots, R_i - 1, \tag{5b}$$

$$\sum_{j \in \mathcal{J}_i} e_{ijr} \le \sum_{j \in \mathcal{J}_i} h_{ijr}, \forall i \in \mathcal{I}, \forall r = 0, 1, \cdots, R_i - 1, \tag{6}$$

$$x_j, h_{ijr}, e_{ijr} \in \{0,1\}, \forall i \in \mathcal{I}, \forall j \in \mathcal{J}_i, \forall r = 0, 1, \cdots, R_i - 1. \tag{7}$$

Constraint (2) enforces the budget limit, while constraints (3) - (7) postulate the valid assignment rule. Constraints (3) (or (4)) ensure that each installed sensor is assigned to each of its corresponding paths at one and only one head (or rear) assignment level. Constraints (5) and (6) indicate that no more than one head or rear sensor is assigned to

each path at each level, and each rear assignment must be accompanied by a head assignment. Constraints (6) also imply that for each path *i*, all the implemented head assignment levels, $\{r \mid \sum_{j \in \mathcal{J}_i} h_{ijr} = 1\}$, start from 0 and form a consecutive sequence. Constraints (7) postulate all decision variables to be binary.

The following proposition reveals the relationship between the above formulation and the valid assignment rule.

Proposition 1: The optimal solution to the TSC problem (1)-(7) satisfies the valid assignment.

Proof. Let $\mathbf{x}^*$, $\mathbf{h}^*$, $\mathbf{e}^*$ denote the optimal solution to TSC. Again locations with installed sensors on each path *i* are indexed with $\{j_0^i, j_1^i, ..., j_{S_i-1}^i\}$ from upstream to downstream. Let $\mathcal{R}_i^h$ denote the set of all implemented head assignment levels to i; i.e., $\mathcal{R}_i^h := \{r \mid \sum_{j \in \mathcal{J}_i} h_{ijr} = 1\}$. Similarly, let $\mathcal{R}_i^e := \{r \mid \sum_{j \in \mathcal{J}_i} e_{ijr} = 1\}$. For the case of $q = 0$, there is no failure and only the level-0 assignment affects the objective value. It is obvious that the optimal solution enforces all non-trivial assignments (at level-0) to be consistent with the valid assignment rule.

Now we consider the case with $q > 0$. Since each installed sensor on i corresponds to only one implemented head (or rear) assignment level (from (3) and (4)) and different sensor cannot have the same head (or rear) assignment level (from (5) and (6)), it is obvious that $|\mathcal{R}_i^h| = |\mathcal{R}_i^e| = S_i$.

For the head assignment, due to constraints (5), $\mathcal{R}_i^h$ contains a sequence of levels from 0 to $S_i - 1$. Due to constraints (6), $\mathcal{R}_i^e \subseteq \mathcal{R}_i^h$. Thus $\mathcal{R}_i^h = \mathcal{R}_i^e = \{0, 1, \cdots, S_i - 1\}$, and we denote them by $\mathcal{R}_i$. Therefore on path *i*, each sensor j_s^i is labeled with a unique head (or rear) assignment level in $\mathcal{R}_i$. At optimality, a more upstream sensor shall have a lower head assignment level and a higher rear assignment level. Thus j_s^i corresponds to

the level-s head assignment and the level-$(S_i - 1 - s)$ rear assignment to i, which is the valid assignment rule.

It shall be noted that the TSC modal can be easily adapted for cases where existing installations are already present (Ehlert et al., 2006). We simply enforce $x_j = 1$ if a sensor is already installed at location j; the model still has the same structure and complexity.

2.2   *Solution approach*

We have built a linear integer mathematical program that determines sensor deployment to optimize traffic surveillance benefits from both individual sensor flow coverage (e.g., for traffic volume statistics) and synthesized sensors (e.g., for travel time estimation). This model builds on the reliable facility location literature and allows sensors to be subject to probabilistic failures (e.g., due to technical flaws or environmental hazards). The formulated problem is complex by nature, which imposes a prohibitive computational burden on solving this problem with commercial solvers (e.g., CPLEX). We therefore propose customized greedy and Lagrangian relaxation algorithms to solve the problem efficiently. These proposed algorithms are applied to this project to yield very good results, while CPLEX often has difficulty in solving most of tested instances. Those who are interested in details are referred to Li and Ouyang (2009).

TSC is NP-hard because the maximal covering problem is a special case of TSC (with $b_t = 0$ and $q = 0$). As we will show in Section 4, commercial optimization software (e.g., CPLEX) would work well only for small-scale instances but it usually runs into difficulty when problem size increases. We hence propose customized algorithms to obtain near-optimal solutions for large-scale problems. The first algorithm is based on a simple greedy heuristic, which can yield good solutions for many realistic applications. But it does not provide information on how close these solutions are from the true optima. Hence we propose a second algorithm based on Lagrangian relaxation (LR), which provides not only good feasible solutions but also optimality gaps.

2.2.1 **Greedy algorithm**

The greedy algorithm for TSC simply selects sensor locations sequentially based on the best marginal increase of objective (1), until all N installation locations have been selected. The exact steps are as follows.

Step 0: Initialization. Let the set of selected location indices $Q := \varnothing$ and the iteration index $n := 1$. Set $x_j = 0, \forall j \in \mathcal{J}$;

Step 1: Search for the nth location that will bring the maximum marginal improvement of objective n^{th}; i.e., select $j^* = \arg\max_{k \in \mathcal{J} \backslash Q} \{z(\mathbf{x}') : x'_j = 1, \text{ iff } j \in Q \bigcup \{k\}\}$. The corresponding marginal objective improvement is denoted by $\rho_n := z(\mathbf{x}') - z(\mathbf{x})$, where $x'_j = 1$, iff $j \in Q \bigcup \{j^*\}$. Let $x_{j^*} = 1$ and $Q = Q \bigcup \{j^*\}$.

Setp 2: If $n=N$, stop and return $\mathbf{x}$ and the corresponding objective value $\sum_{n=1}^{N} \rho_n$; otherwise, $n = n+1$, and go to step 1.

Greedy heuristic is widely applied to many practical problems not only because of its simplicity but also due to its reasonable practical performance. For example, in case of the classic maximal covering problem (a special case of TSC where $q=0$ and $b_i=0$), Feige (1998) proved that the objective value of any greedy solution is no smaller than $(1-1/e)$ of the true optimum; i.e., the approximation ratio is $e/(e-1)$. More importantly, no known polynomial-time algorithm can beat the greedy algorithm in terms of this approximation ratio bound (Feige, 1998). We can obtain a similar approximation ratio for the maximal covering problem with probabilistic facility failures (a special case of TSC where $b_t = 0$ and $q > 0$).

For general TSC, however, the approximation ratio of the proposed greedy algorithm is not bounded. This can be seen from the following simple example. Suppose a network has three nodes $\mathcal{J} = \{1, 2, 3\}$, two links $\{(1,2),(2,3)\}$, and two consecutive O-D flow paths, i.e., $\mathcal{I} = \{a,b\}$ with $f_a = 0, f_b = 1$, and $\mathcal{J}_a = \{1,2\}$ and $\mathcal{J}_b = \{2,3\}$. If $b_c = 0$,

$b_t > 0$ and $N = 2$, a possible solution from the greedy algorithm is $Q = \{1, 2\}$, which yields $z(\mathbf{x}) = 0$. Yet the optimal solution is obviously $Q = \{2, 3\}$, which gives a positive objective value. Hence, the proposed greedy algorithm for TSC does not have a performance bound, and we propose an LR-based algorithm in the next section.

2.2.2 LR-based Algorithm

2.2.2.1 Relaxed subproblems and bounds

We relax constraints (5) and (6), and add them to the objective (1) with nonnegative Lagrangian multipliers $\lambda = \{\lambda_{ir}\}$ and $\gamma = \{\gamma_{ir}\}$, respectively. The relaxed TSC (RTSC) becomes:

$$(\text{RTSC}) \quad \min_{\lambda, \gamma \geq 0} z_R(\lambda, \gamma) := \max_{\mathbf{x}, \mathbf{h}, \mathbf{e}} \left[\sum_{i \in \mathcal{I}} \sum_{j \in \mathcal{J}_i} \sum_{r=0}^{R_i - 1} (H_{ijr} h_{ijr} + E_{ijr} e_{ijr}) + \sum_{i \in \mathcal{I}} \lambda_{i0} \right] \quad (8)$$

$$\text{s.t. (2)-(4) and (7),}$$

where the benefit of an installation at location j as a level-r head sensor for any $i \in \mathcal{I}_j$ is

$$H_{ijr} = \begin{cases} -q^r(1-q)f_i b_t m_{ij} - \lambda_{ir} + \lambda_{i(r+1)} + \gamma_{ir}, & r = 0, 1, \cdots, R_i - 2; \\ -q^r(1-q)f_i b_t m_{ij} - \lambda_{ir} + \gamma_{ir}, & r = R_i - 1, \end{cases} \quad (9)$$

and the benefit of this installation as a level-r rear sensor is

$$E_{ijr} = q^r(1-q)f_i(b_t m_{ij} + b_c) - \gamma_{ir}. \quad (10)$$

For any given λ and γ, the exact value of $z_R(\lambda, \gamma)$ provides an upper bound of (1), and it can be obtained from the following decomposition scheme. When (5) and (6) are relaxed, assignments are no longer dependent across j. Constraints (3) require that the hear assignment of each j with sensor installed is conducted at exactly one level for each

$i \in \mathcal{I}_j$. Thus to achieve the optimal benefit, j is assigned to i as a head sensor at the level corresponding to the maximum H_{ijr} across all *r*. Similarly, the corresponding rear assignment level is chosen to maximize E_{ijr} across all *r*. Therefore, in RTSC, the contribution of installing a sensor at j, in terms of objective (8), is

$$B_j = \sum_{i \in I_j} [\max_r (H_{ijr}) + \max_r (E_{ijr})] \tag{11}$$

Obviously, the optimal solution to (8) is to set $x_j = 1$ for the *N* locations with the largest B_j values, and accordingly, set $h_{ijr} = 1$ (or $e_{ijr} = 1$) if $x_j = 1$ and r maximizes H_{ijr} (or E_{ijr}) across all r.2 Then the optimal objective value of RTSC is

$$z_R(\lambda, \gamma) = \sum_{j \in \mathcal{J}} B_j x_j + \sum_{i \in \mathcal{I}} \lambda_{i0} \tag{12}$$

Since the solution obtained from the above procedure is probably not feasible to the original TSC problem, heuristic methods are used to construct a feasible solution. Although such constructive heuristics do not guarantee the exact optimal solution, previous experiments (Cornuejols et al., 1977; Caprara et al., 1999) yield very good feasible, often exactly optimal, solutions (and tight lower bounds of the original objectives) if the Lagrangian multipliers are near convergence. One simple heuristic is that we install all facilities that are obtained from RTSC, and then apply the valid assignment rule to determine the feasible **h** and **e** accordingly. If the lower bound equals the upper bound at any iteration, then the optimal solution is found. Otherwise, the difference between these bounds provides an optimality gap - the difference between the true optimum and the feasible solution is sure to be no larger than this gap.

For the classic maximal covering problem (*q*=0and *b_i*=0), Cornuejols et al. (1977) proved that the relative gap between the optimal LR solution and the optimal TSC

---

[2] Ties can be broken arbitrarily

solution is bounded by 1/e. This bound holds for more general problems with positive failure probability $q>0$.

It should be noted that the computational time for solving the RTSC problem (8) and for obtaining an feasible solution are bounded by $O(N \cdot |\mathcal{I}| + |\mathcal{J}| \sum_{i \in \mathcal{I}} R_i)$ and $O(N \cdot |\mathcal{I}|)$, respectively.

2.2.2.2 Multiplier updating

Function $z_R(\lambda, \gamma)$ is known to be convex over λ and γ. RTSC can be solved with an iterative subgradient search. We update λ and γ iteratively to find the tightest upper bound $\min_{\lambda, \gamma \geq 0} z_R(\lambda, \gamma)$. We add subscript k to distinguish variables in iteration k. The initial values of the multipliers are obtained with heuristics (e.g., the dual solution to the linear relaxation of the original problem). At the end of each iteration, multipliers are updated as follows.

$$\lambda_{ir}^{k+1} = \max\left(0, \lambda_{ir}^k + t^k \Delta \lambda_{ir}^k\right), \forall i \in \mathcal{I}, \forall r = 0, 1, \cdots, R_i - 1,$$

$$\gamma_{ir}^{k+1} = \max\left(0, \gamma_{ir}^k + t^k \Delta \gamma_{ir}^k\right), \forall i \in \mathcal{I}, \forall r = 0, 1, \cdots, R_i - 1,$$

where the subgradients are

$$\Delta \lambda_{ir}^k := \sum_{j \in \mathcal{J}_i} h_{ijr} - \begin{cases} 1, & r = 0 \\ \sum_{j \in \mathcal{J}_i} h_{ij(r-1)}, & \text{otherwise} \end{cases},$$

and $\Delta \gamma_{ir}^k := \sum_{j \in \mathcal{J}_i} (e_{ijr} - h_{ijr})$. Step size t_k is usually set to

$$t^k = \frac{\mu^k (z_R(\lambda^k, \gamma^k) - z^{LB})}{\sum_{i \in \mathcal{I}} \sum_{r=0}^{R_i - 1} \left[(\Delta \lambda_{ir}^k)^2 + (\Delta \gamma_{ir}^k)^2 \right]},$$

where μ^k is a control scaler, and z^{LB} is the objective value of the best-known feasible solution. Traditionally, control scaler μ^k is determined by setting $\mu^0 = 2$ and halving μ^k if $z_R(\lambda^k, \gamma^k)$ is not improved after a fixed number of iterations (Fisher, 1981). This approach is modified by (Fisher, 1981) Caprara et al. (1999) for faster convergence. The idea is to set $\mu^0 = 0.1$, and compare the best and worst values of $z_R(\lambda^k, \gamma^k)$ in every certain number (e.g., 20) of iterations: decrease μ^k if the difference is greater than a larger threshold (e.g., 1%) and increase μ^k if the difference is less than a smaller threshold (e.g., 0.1%). In our case study, we use the traditional approach when multipliers are far from their optimal values and then switch to the second approach near convergence.

In principle, the LR algorithm is terminated if one of the following conditions is satisfied: (i) the lower bound equals the upper bound, (ii) the optimality gap stops reducing, and (iii) the solution time exceeds a reasonable limit. Our experience shows that condition (ii) terminates the algorithm most of the time. In case that happens, we may use the following branch and bound procedure to further reduce the optimality gap.

2.2.2.3 Branch and bound

If the aforementioned LR algorithm ends up having a non-zero optimality gap, we implement the LR algorithm into a branch and bound framework. We branch on variables $\mathbf{x}$ in a depth-first manner, and use a greedy heuristic to choose the next variable x_j for branching: installation at j shall bring in the greatest increase of the objective value (1) given the variables that have already been branched. We branch each variable first to 1 (enforcing installation) and then to 0 (forbidding installation). At each node, we run the LR algorithm to determine the lower and upper bounds, while extra constraints for already-branched variables are exerted. If the upper bound is lower than the best feasible solution so far, the node no longer has potential and is trimmed. If the current node has already had N enforced or $|\mathcal{J}| - N$ forbidden installations, only one non-trivial feasible

solution exists and is returned as both the lower and the upper bounds. At each branching, the multipliers of a parent node are passed down to its child nodes as their initial multipliers.

2.3   *Algorithm test*

The Sioux-Falls network has 24 vertices and 76 links, as shown in Figure 2.1. Assume that all the vertices are candidate locations, i.e., $|\mathcal{J}| = 24$. There are 528 traffic O-D pairs. For simplicity, we assume that each O-D pair only has one flow path that is determined by the shortest path algorithm5, and hence $|\mathcal{I}| = 528$. Assume too that the sensor at a node can detect all traffic passing that node from different directions.
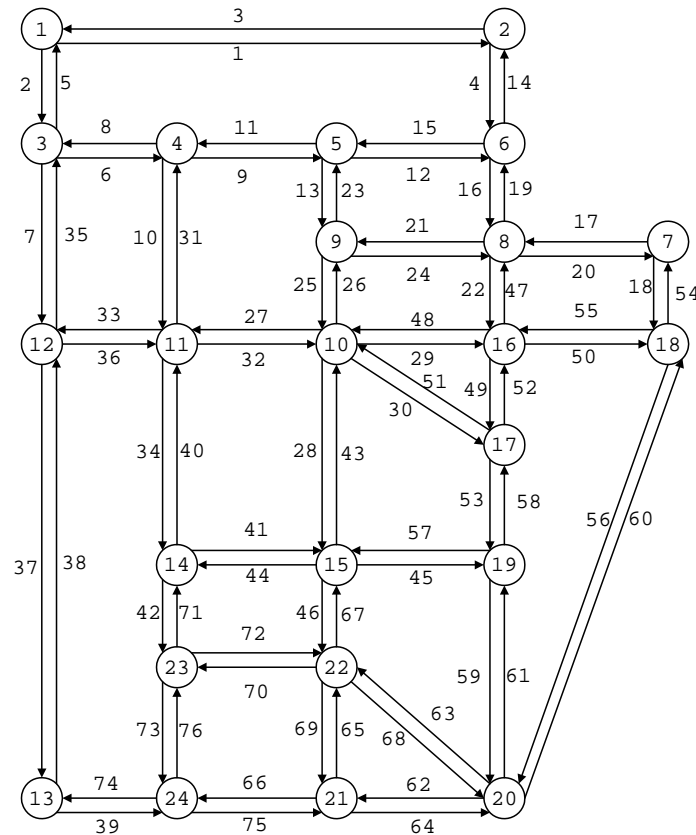

Figure 2.1. The Sioux-Falls test network. (Source: http://www.bgu.ac.il/~bargera/tntp/.)

The experiments are implemented on a PC with 2.0 GHz CPU and 2 GB memory. We set a solution time limit of 1800 seconds, and run a series of instances $b_t = 1$, $b_c \in \{0,1,10\}$, $N \in \{3,5,7\}$, and $q \in \{0,0.05,0.2,0.5\}$. The results are summarized in Table 1. In this table, denote the optimal objective value for the LR-based algorithm by z^*, the solution time by T, and the optimality gap by ϵ. The objective value found by the greedy algorithm by z^G. For comparison, we solve the same instances with commercial software CPLEX, and let z^C, T^C and ϵ^C be the objective value, the solution time and the residual optimality gap, respectively. Let $\alpha := b_t /(b_t + b_c)$ be an indicator of the relative importance of path coverage benefit.[3] As we can see, the LR-based algorithm found optimal solutions for almost all the instances ($\epsilon = 0\%$). CPLEX has a comparable performance only when α is small (i.e., flow coverage dominates). Otherwise, the performance of CPLEX is significantly worse than the LR-based algorithm: CPLEX cannot find the optimal solution within 1800 seconds for many instances, and sometimes it even cannot find a meaningful feasible solution (where $z^C = 0$ or $\epsilon^C = \text{INF}\%$). The greedy algorithm finds a good feasible solution (i.e., $z^G \approx z^*$) when α is small. For most instances with $\alpha = 1$, however, the results from the greedy algorithm are quite far from the optima. This implies that the greedy algorithm does not work as well when path coverage is the dominating objective. This is probably because a sensor's contribution to path coverage highly depends on other sensors' locations.

---

[3] Note that once α is fixed, scaling the value of b_t (or b_c) does not affect the optimal sensor deployment.
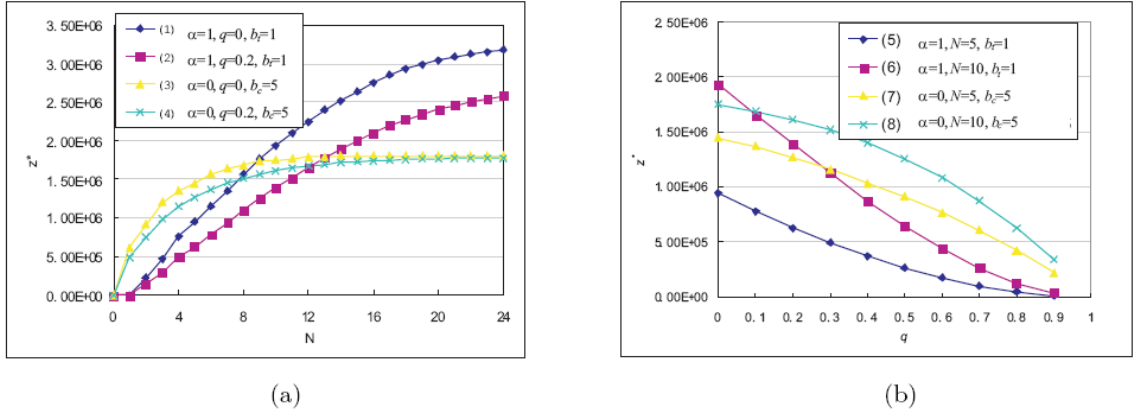
Figure 2.2. Relationship between *N*, *q* and z^* for the Sioux-Falls network.

In Table 1, z^* increases with *N* and decreases with *q*, as expected. Figure 2.2 further reveals their relationships by plotting z^* over *N* and *q* for different parameter values. In Figure 2.2a, curves 1 and 2 are for path coverage only ($\alpha = 1$) and curves 3 and 4 are for flow coverage only ($\alpha = 0$). We see that curves 3 and 4 quickly flatten out while curves 1 and 2 almost linearly increase until *N* is close to $|\mathcal{J}|$. This suggests that path coverage benefit is more sensitive to value of *N*. This is probably because the marginal path coverage benefit depends not only on the additional installation itself, but also on other installations that form pairs with the additional one. The differences between curves 1 and 2, and that between 3 and 4 represent the expected coverage loss due to probabilistic sensor failures. Although such loss is small for flow coverage, it is significant for path coverage. This is further confirmed by Figure 2.2b which shows how z^* varies with q. Curves 5 and 6 are for path coverage while curves 7 and 8 are for flow coverage. We see that when q is not too large (e.g., q<0.5, which is true for most real-world cases), curves 5 and 6 drop much faster than curves 7 and 8. This confirms the observation that the benefit loss due to failures is more significant for path coverage. In this case, sensor failures should be addressed carefully. It is also interesting to notice that curves 5 and 6 are rather convex while 7 and 8 are rather concave, indicating opposite sensitivity behaviors in different *q* value ranges.

Table 1 Results for Sioux-Falls test network

#	N	q	b_e	α	z^G	z^*	z^C	T/s	T^C/s	ϵ	ϵ^C
1	3	0	0	1.00	230600	469200	469200	59	66	0 %	0 %
2	3	0	1	0.50	692800	692800	692800	8	53	0 %	0 %
3	3	0	5	0.17	1.59E+06	1.59E+06	1.59E+06	1	1	0 %	0 %
4	3	0.05	0	1.00	208117	423453	423453	60	414	0 %	0.01 %
5	3	0.05	1	0.50	640371	640371	640371	8	288	0 %	0.01 %
6	3	0.05	5	0.17	1.51E+06	1.51E+06	1.51E+06	2	1	0 %	0 %
7	3	0.2	0	1.00	150426	300288	287168	73	>1800	0 %	18.29 %
8	3	0.2	1	0.50	494320	494320	494320	11	341	0 %	0.01 %
9	3	0.2	5	0.17	1.27E+06	1.27E+06	1.27E+06	2	1	0 %	0 %
10	3	0.5	0	1.00	62000	119838	92925	270	>1800	0 %	86.68 %
11	3	0.5	1	0.50	252775	252775	252775	29	>1800	0 %	3.24 %
12	3	0.5	5	0.17	794675	794675	794675	1	1	0 %	0 %
13	5	0	0	1.00	662800	947800	947800	44	113	0 %	0 %
14	5	0	1	0.50	1.22E+06	1.22E+06	1.22E+06	23	107	0 %	0 %
15	5	0	5	0.17	2.31E+06	2.31E+06	2.31E+06	6	8	0 %	0 %
16	5	0.05	0	1.00	607112	861901	861901	52	>1800	0 %	0.97 %
17	5	0.05	1	0.50	1.13E+06	1.13E+06	1.13E+06	16	270	0 %	0.01 %
18	5	0.05	5	0.17	2.19E+06	2.19E+06	2.19E+06	5	13	0 %	0.01 %
19	5	0.2	0	1.00	507213	625062	588058	123	>1800	0 %	17.26 %
20	5	0.2	1	0.50	872339	872339	865773	35	>1800	0 %	2.05 %
21	5	0.2	5	0.17	1.87E+06	1.87E+06	1.87E+06	4	5	0 %	0 %
22	5	0.5	0	1.00	213788	266725	0	642	>1800	0 %	INF %
23	5	0.5	1	0.50	449163	449163	443650	81	>1800	0 %	5.82 %
24	5	0.5	5	0.17	1.18E+06	1.18E+06	1.18E+06	2	2	0 %	0 %
25	7	0	0	1.00	1.28E+06	1.35E+06	1.35E+06	110	125	0 %	0 %
26	7	0	1	0.50	1.65E+06	1.65E+06	1.65E+06	59	176	0 %	0.01 %
27	7	0	5	0.17	2.92E+06	2.92E+06	2.92E+06	30	1	0 %	0 %
28	7	0.05	0	1.00	1.18E+06	1.24E+06	1.24E+06	124	1783	0 %	0.01 %
29	7	0.05	1	0.50	1.54E+06	1.54E+06	1.54E+06	56	599	0 %	0.01 %
30	7	0.05	5	0.17	2.78E+06	2.78E+06	2.78E+06	9	4	0 %	0 %
31	7	0.2	0	1.00	897554	936031	0	376	>1800	0 %	INF %
32	7	0.2	1	0.50	1.22E+06	1.22E+06	1.21E+06	111	>1800	0 %	1.04 %
33	7	0.2	5	0.17	2.36E+06	2.36E+06	2.36E+06	8	7	0 %	0 %
34	7	0.5	0	1.00	388425	411363	0	1800	>1800	26 %	INF %
35	7	0.5	1	0.50	622325	625738	0	576	>1800	0 %	INF %
36	7	0.5	5	0.17	1.48E+06	1.48E+06	1.48E+06	8	7	0 %	0 %

Figure 2.3 shows the impact of α and q on the optimal sensor deployment. The link width illustrates flow volumes. The dark nodes are the optimal installation locations, which are generally at places with heavy traffic. The optimal deployment for path coverage ($\alpha = 1$) is more spread-out than that for flow coverage ($\alpha = 0$). This is intuitive

because more scattered sensor pairs can cover longer paths. On the other hand, higher failure probability generally leads to a higher degree of sensor clustering.
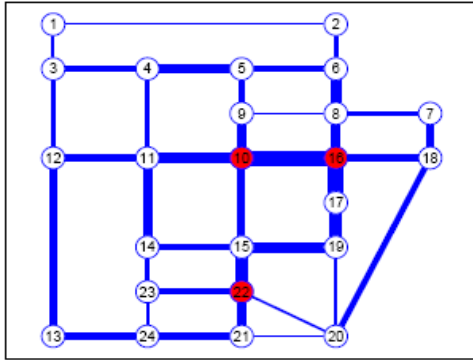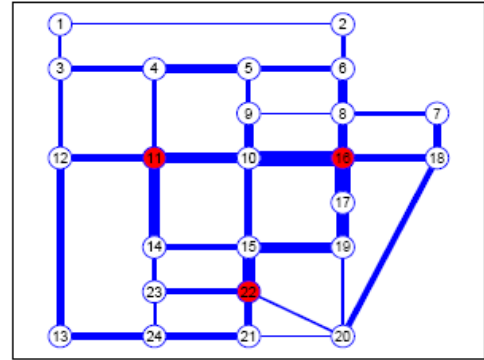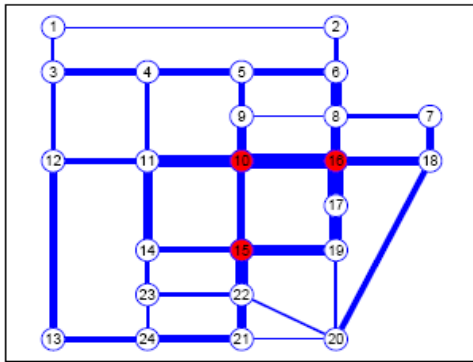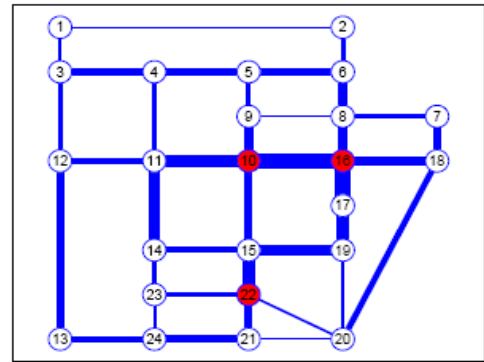

(a) $\alpha = 0$ and $q = 0$

(b) $\alpha = 1$ and $q = 0$

(c) $\alpha = 0$ and $q = 0.2$

(d) $\alpha = 1$ and $q = 0.2$

Figure 2.3. Optimal deployment of N=3 installations in the Sioux-Falls network.

CHAPTER 3. CASE STUDY: THE INDOT-MAINTAINABLE NETWORK

Chapter 3 discusses the application of the proposed model to a large-scale real problem, the Chicago intermodal network. Section 3.1 introduces how to obtain input data by integrating multiple data sources. Heuristics are taken to extract detailed information from limited data with coarse granularity. Section 3.2 analyzes solutions with different algorithms for a set of instances. Managerial insights are drawn on how coverage measure and failure probabilities influence optimal sensor deployment.

3.1 *Data preparation*

Collecting accurate and quality data is very important to illustrate that the proposed model and solution techniques can be applied to realistic scenarios. Without data or with invalid data, the results of the experiments could be misleading. The data preparation efforts consist of network portion and freight movement portion.

Network

We first had to figure out the network system in a simple and realistic way, and to transform it in a mathematical representation. In Chicago, intermodal traffic is transported through two networks: highway and rail. Unlike the highway network system which is easily recognizable, rail network system is more complicated and harder to access. Besides, there were simply not enough data available for rail traffic to figure out complete picture of intermodal traffic movement. Our team decided to focus our network on highway network and rail terminals where highway and rail interchange occurs. Here are some of concepts and terms we defined regarding the network.

1. Access Point – An access point is an entrance point that connects the highway network in Chicago and the outside world. There are 8 access points in the Chicago network, and these points basically define the network boundary.

2. Conjunction – A conjunction is an interchange of two highways. Conjunctions play an important role in this network as they represent the local population. To represent Chicago population, we assumed that conjunctions are dominant over local highway networks meaning conjunctions absorb all local population. Basically, conjunctions function as local exits as we do not consider any local exits.

   o Sensors will be deployed at conjunctions: Logically, it makes sense to install sensors at conjunctions rather than in the middle of highway since traffic only can change their route at conjunctions.

3. Terminals – A terminal is basically a rail yard where freight transition occurs between rail and truck. There are 17 terminals in Chicago land area, and their locations are represented at the nearest highway exit for the purpose of not dealing with local road networks.

4. Network Representation (Sheffi, 1985) – Recalling the limited effectiveness range of RFID sensors (~31ft), one installation of RFID detection structure can only cover one travel bound on a highway. In other words, to cover the entire conjunction with RFID, all four directions of the conjunction needs to be installed with RFID detection separately. To break down a conjunction, we used the network representation approach developed by Yosef Sheffi in Urban Transportation Networks in 1985. Figure 3.1 explains how a conjunction breaks down into multiple nodes and directions.
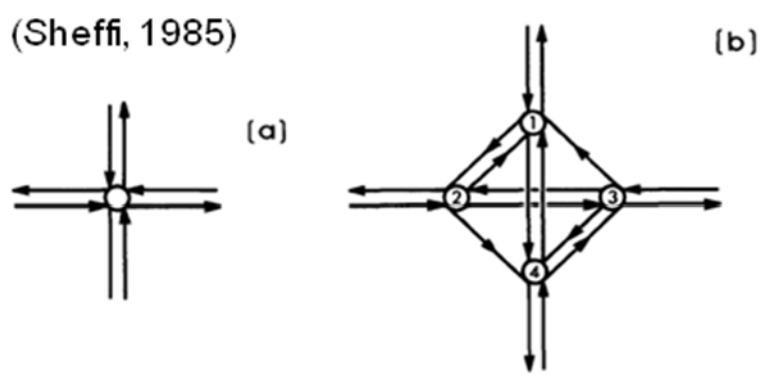
Figure 1.5 Network representation of the intersection in Figure 1.4: (a) representing the intersection as a node; (b) a detailed intersection representation.

Figure 3.1. Network representation of an intersection

When a conjunction is broken, it creates 4 nodes, each representing a traffic direction. Using this concept, we broke down all 21 conjunctions to obtain 72 equivalent network nodes.
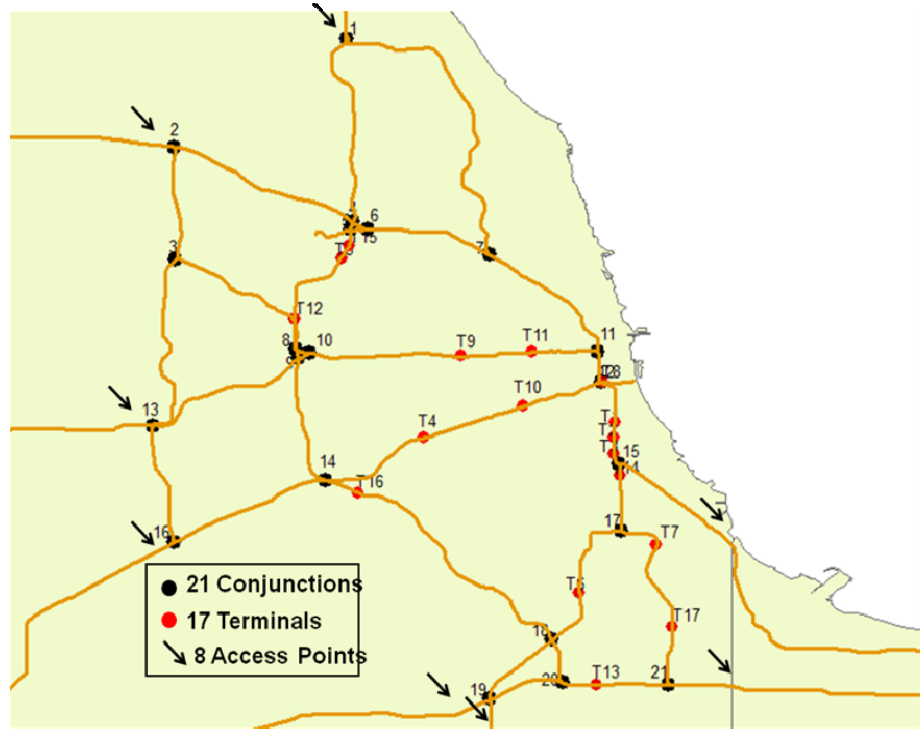

Figure 3.2. Network diagram of Chicago

Figure 3.2 is the network diagram of Chicago highway and terminals. It shows all the locations of conjunctions, terminals, and access points. After the coding of the network, we obtained 89 total nodes, 353 total links, and 1046 O-D flows.

Freight Movement

Understanding the movement of intermodal freight traffic is a crucial part of the data preparation efforts. The primary data source we used was from the website of Bureau of Transportation Statistics.[4] Given data that describes only a small portion of the entire traffic, we had to utilize the data as much as possible to draw the most realistic picture as possible. The data summary is shown in Table 2.

Table 2. Chicago freight volume table from Bureau of Transportation Statistics

(unit: thousand tons)	Inbound	Outbound
All Modes	**384,554**	**398,993**
Single Mode	**371,023**	**381,750**
Truck	**312,279**	**294,611**
Truck: Outer States	**117,289**	**87,778**
Rail	**34,343**	**43,957**
Multi Modes	**5,926**	**9,864**

1. Single Mode – Single mode traffic describes the freight traffic that is transported by truck only and has Chicago as destination or origin. Inbound single mode

---

traffic originates from other states and crosses an access point to enter the network and ends up at local Chicago exits represented by conjunctions. Outbound traffic starts at conjunctions and ends up in outer states. These traffic volumes are obtained at the website of Bureau of Transportation Statistics under Commodity Flow Survey 2002. The route that single mode traffic chooses is based on the shortest path between Chicago and the metropolitan city of the state of origin, and we assign that traffic volume to the access point they cross. After assigning all the volume to the access points, then we use the gravity model method to distribute the volume to 21 conjunctions according to nearby population weights.

2. Intermodal – Intermodal traffic here describes freight traffic that travels on both rail and highway. Inbound traffic travels by rail and gets dropped off at terminals within the network. Then they travel from terminals to conjunctions by truck, and that is the only part we are concerned about.

3. There are several assumptions we made to simplify the difficulty associated with data scarcity. First, we ignored the traffic that goes through Chicago. Given limited data, it was almost impossible to distinguish through traffic from others. Moreover, as we suspected that most of through traffic would take more of peripheral routes around metropolitan area rather than going through them, we decided to take them out of the picture. Another area of uncertainty was the rail terminal transaction freight volumes. Rail freight tonnage numbers are given, but there is simply no data available for us to track down how the freight is distributed or which route they take. Thus, we assumed that all rail freight volume that is transported to the terminal is destined to conjunctions and vice versa.
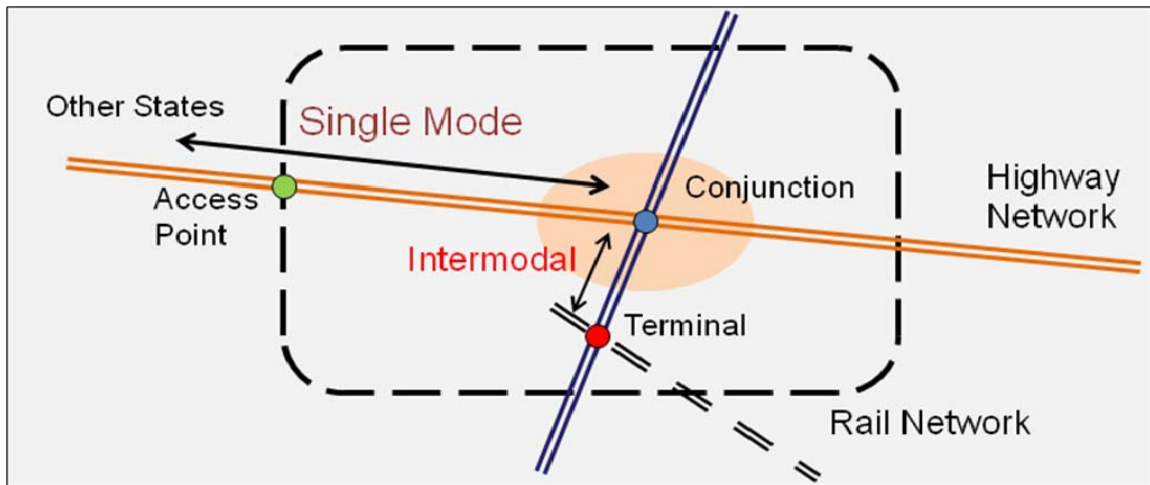
Figure 3.3. Network and freight movement diagram

Figure 3.3 illustrates the Chicago network and the all the freight movements around the network.

3.2   *Results*

We conducted a set of experiments on a PC with 2.0 GHz CPU and 2 GB memory for the greedy algorithm, the LR-based algorithm, and CPLEX. The solution time limit is set to be 1200 seconds. We have run a series of instances for $b_t \in \{0,1\}$, $b_c \in \{0,1,4\}$, $N \in \{10, 20, 30\}$, and $q \in \{0, 0.2, 0.5\}$. The results are summarized in Table 3. Due to the increased problem size, CPLEX cannot even get a meaningful feasible solution for most instances. The LR-based algorithm always yields a near-optimum solution with a reasonable residual gap ($\leq 15\%$). From our experiments, the difference between the near-optimal solution and the optimum is often much smaller than the residual gap. Thus these solutions are suitable for engineering practice.

Table 3. Results for Chicago intermodal network

#	N	q	b_c	α	z^G	z^*	z^C	T/s	T^C/s	ϵ	ϵ^C
1	10	0	0	1	3.80E+06	4.22E+06	1.95E+06	1200	1200	5 %	120 %
2	10	0	1	0.5	4.12E+06	4.48E+06	0	1200	1200	4 %	INF %
3	10	0	4	0.2	4.84E+06	5.28E+06	0	1200	1200	3 %	INF %
4	10	0	1	0	274219	275462	275461	1200	1200	5 %	0 %
5	10	0.2	0	1	2.93E+06	3.00E+06	0	1200	1200	15 %	INF %
6	10	0.2	1	0.5	3.14E+06	3.25E+06	0	1200	1200	12 %	INF %
7	10	0.2	4	0.2	3.82E+06	3.99E+06	0	1200	1200	9 %	INF %
8	10	0.2	1	0	253215	253408	253408	1200	48	5 %	0 %
9	10	0.5	0	1	1.57E+06	1.69E+06	0	1200	1200	15 %	INF %
10	10	0.5	1	0.5	1.85E+06	1.85E+06	0	1200	1200	14 %	INF %
11	10	0.5	4	0.2	2.38E+06	2.41E+06	0	1200	1200	9 %	INF %
12	10	0.5	1	0	203567	203567	203567	1200	6	7 %	0 %
13	20	0	0	1	5.60E+06	5.78E+06	5.82E+06	1200	838	10 %	0 %
14	20	0	1	0.5	6.01E+06	6.08E+06	6.10E+06	1200	820	10 %	0 %
15	20	0	4	0.2	6.86E+06	6.91E+06	6.94E+06	1200	608	10 %	0 %
16	20	0	1	0	283361	283361	0	1200	1200	9 %	INF %
17	20	0.2	0	1	4.71E+06	4.75E+06	0	1200	1200	9 %	INF %
18	20	0.2	1	0.5	4.95E+06	5.02E+06	0	1200	1200	8 %	INF %
19	20	0.2	4	0.2	5.79E+06	5.84E+06	0	1200	1200	7 %	INF %
20	20	0.2	1	0	274962	275057	274480	1200	516	7 %	0 %
21	20	0.5	0	1	2.93E+06	2.99E+06	0	1200	1200	5 %	INF %
22	20	0.5	1	0.5	3.19E+06	3.22E+06	0	1200	1200	5 %	INF %
23	20	0.5	4	0.2	3.90E+06	3.93E+06	0	1200	1200	3 %	INF %
24	20	0.5	1	0	244680	244680	240456	1200	49	7 %	2 %

The following comparisons helped us draw managerial insights into the sensor deployment problem.

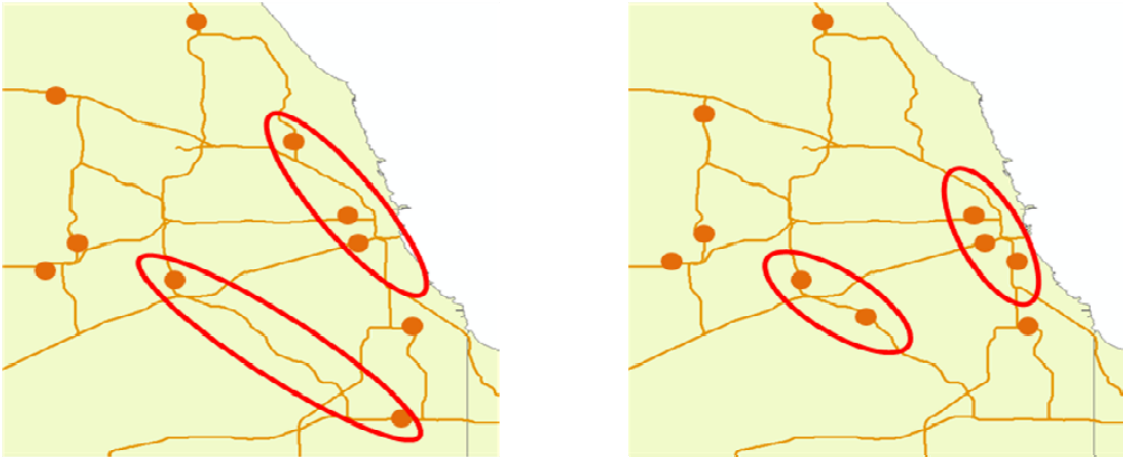   a. Varying sensor failure probabilities at flow coverage with 10 sensors (Figure 3.4)

Figure 3.4. Sensor deployment with failure probability of 0% and 20%

When the sensors are 100% reliable (i.e. 0% failure probability), 10 sensors will have 96.8% coverage rate; under 20% failure rate, the coverage rate drops to 89.4%. From the figures, we also see that the sensor deployment at 20% failure probability shows more scattering pattern of sensors than 0% failure probability. This is intuitive since with higher failure probability, sensors need to be densely deployed in the central area to back each other up in case one fails.

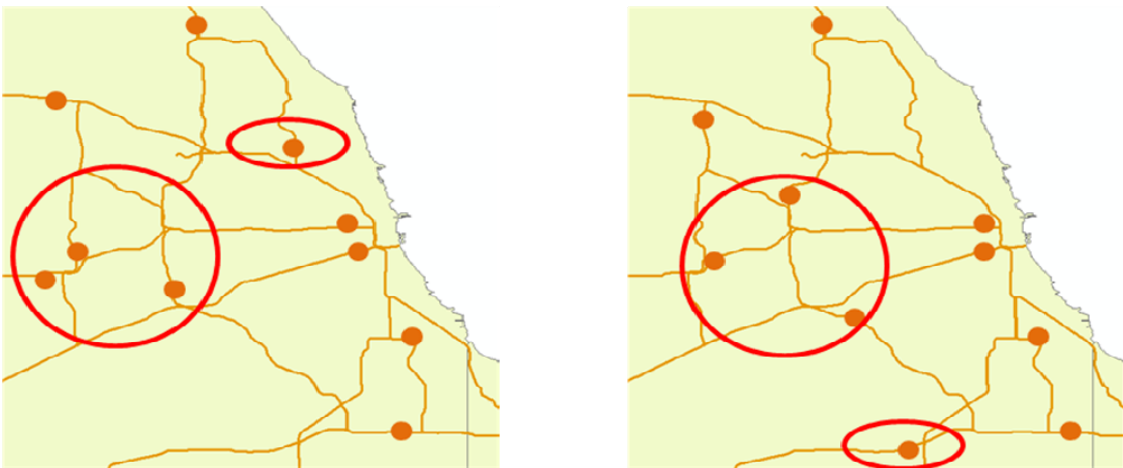b. Flow coverage and path coverage (Figure 3.5)

Figure 3.5. Sensor deployment with flow coverage and path coverage

Then we compared flow and path coverage at 0% failure probability. Path coverage showed a coverage rate of 67.8% which is a lot less than flow coverage. If we compare the two big red circles in the diagram above, we see sensors in the path coverage scenario are more spread apart than ones in flow coverage. Because the nature of path coverage is to cover as much traffic as possible, path coverage scenario tends to prioritize quantity of information over the quality of information.

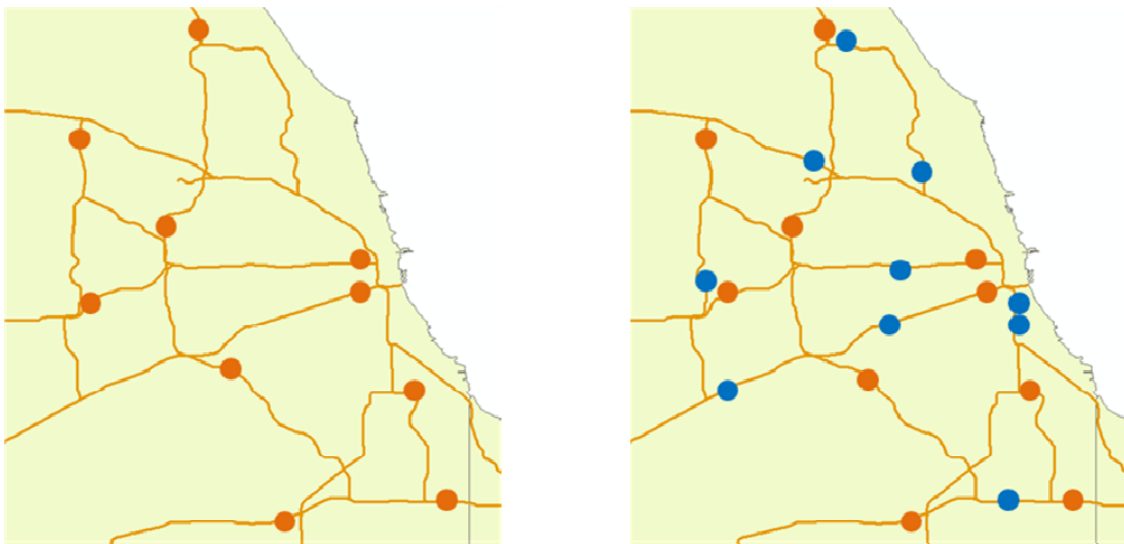   c.   Number of sensors: 10 vs. 20 (Figure 3.6)

Figure 3.6. Sensor deployment with 10 sensors and 20 sensors

Finally, we compared 10 sensors versus 20 sensors on path coverage. Blue dots on right diagram shows 10 new added sensors onto the original network. The coverage rate is 67.8% for 10 sensors and 92.3% for 20 sensors, and it is obvious that more sensors improve the coverage rate of the network.
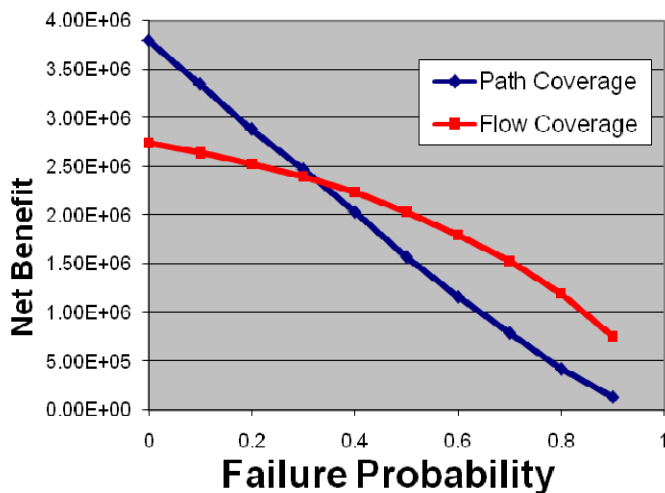
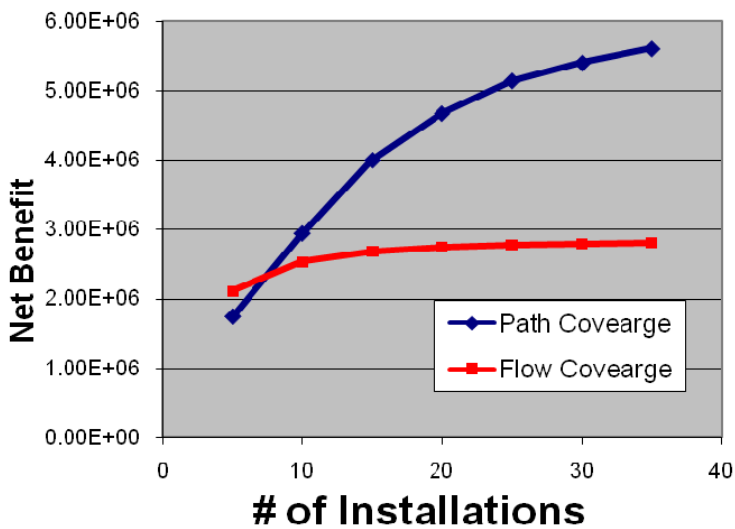Figure 3.7. Failure probability vs. net benefit

Figure 3.8. Number of installations vs. net benefit

Figures 3.7, 3.8 summarize the comparison of flow and path coverage. We graphed the relationships between net benefit and failure probability and one between net benefit and number of sensor installations. The general observation is that net benefit increases at lower sensor probability and higher number of installations. The notable insight we gain from these graphs is that path coverage benefit is much more sensitive

toward any changes in the network. From the graphs, we find that path coverage lines are steeper than flow coverage lines, and that shows the sensitive nature of path coverage.

CHAPTER 4. CONCLUSIONS

This chapter summarizes the research, highlights its contributions, and proposes directions for future research.

4.1 *Summary*

This research addresses a new sensor deployment problem in the context of traffic O-D flow surveillance using vehicle ID inspection technologies (e.g., RFID). In addition to traditional flow coverage benefits based on individual sensors, we investigated the path coverage benefits from synthesizing the multiple sensors in transportation networks. We consider possible sensor disruptions, that are very common for many sensor technologies, yet not well addressed until very recently.

A reliable location design model framework is proposed to optimize sensor deployment benefit. This model considers both flow and path coverage, while allowing for probabilistic sensor failures. A set of efficient algorithms are developed, and tested on a moderate-size problem. We find that the LR-based algorithm has good performance for the tested problems. The greedy-algorithm can yield good solutions if flow coverage benefit is significant.

Then we applies this model to the large-scale Chicago intermodal network. We study both highway and railroad networks and their connections. We describe our efforts to extract detailed input flow data from limited data resources. We examine the qualities of solutions of different algorithms, the best of which (from the LR-based algorithm) are analyzed to draw out managerial insights about sensor deployment. The experiments show that path coverage benefit is more sensitive to sensor failures and installation

budget. It is also found that path coverage tends to spread out sensor locations while high failure probabilities tend to cluster sensors together.

4.2   *Future research directions*

Future work can be conducted in several directions. First of all, the proposed model addresses probabilistic sensor failures but assumes known O-D flow paths. This may be reasonable in the freight operation context but a more comprehensive model that encompasses traffic routing and assignment will be desirable. In addition, the current model assumes all sensor failures are independent with equal probability. Yet more complex sensor failure patterns (e.g, site-dependent and correlated failures) are not uncommon in the real world. Additional work that relaxes these two assumptions is needed. Finally, it will be interesting to explore how alternative traffic surveillance benefits would affect the optimal sensor deployment pattern.

REFERENCES

Renee Meiller, (2007). Midwest transportation coalition addresses regional freight challenges. UW-Madison News. http://www.news.wisc.edu/13852.

Ban, X. J., Herring, R., Margulici, J., Bayen, A. M., 2009. Optimal sensor placement for freeway travel time estimation. Presented at Transportation Research Board 88th Annual Meeting, Jan 2009.

Bianco, L., Confessore, G., Reverberi, P., 2001. A network based model for traffic sensor location with implications on O/D matrix estimates. Transportation Science 35 (1), 50-60.

Caprara, A., Fischetti, M., Toth, P., 1999. A heuristic method for the set covering problem. Operations Research 47 (5), 730-743.

Carbunar, B., Ramanathan, M., Koyuturk, M., Grama, A., Ho®mann, C., 2005. Redundant-reader elimination in RFID systems. In: Proceedings of the 2nd IEEE International Conference on Sensor and Ad Hoc Communications and Networks (SECON). Santa Clara, September 2005.

Cornuejols, G., Fisher, M. L., Nemhauser, G. L., 1977. Location of bank accounts to optimize float: An analytic study of exact and approximate algorithms. Management Science 23 (8), 789-810.

Cui, T., Ouyang, Y., Shen, Z. M., 2009. Reliable facility location under the risk of disruptions. Operations Research (in press).

Daskin, M. S., 1983. A maximum expected covering location model: Formulation, properties and heuristic solution. Transportation Science 17 (1), 48-70.

Ehlert, A., Bell, M. G., Grosso, S., 2006. The optimisation of traffic count locations in road net-works. Transportation Research Part B 40 (6), 460 - 479.

Fei, X., Mahmassani, H. S., 2008. Two-stage stochastic model for sensor location problem in a large-scale network. Presented at Transportation Research Board 87th Annual Meeting, Jan 2008.

Fei, X., Mahmassani, H. S., Eisenman, S. M., 2007. Sensor coverage and location for real-time traffic prediction in large-scale networks. Transportation Research Record 2039 (1), 1-15.

Feige, U., 1998. A threshold of ln n for approximating set cover. Journal of the ACM 45 (4), 314-318.

Fisher, M. L., 1981. The lagrangian relaxation method for solving integer programming problems. Management Science 27 (1), 1-18.

Kerner, B., Rehborn, H., 1996. Experimental properties of complexity in tra±c °ow. Physical Review Letters 53 (5), R4275-R4278.

Li, X., Ouyang, Y., 2009. A continuum approximation approach to reliable facility location design under correlated probabilistic disruptions. Transportation Research Part B (in press).

Li, X., Peng, F., Ouyang, Y., 2009. Measurement and estimation of traffic oscillation properties. Transportation Research Part B (in press).

Ouyang, Y., Li, X., Barkan, C. P. L., Kawprasert, A., Lai, Y.-C., 2009. Optimal locations of railroad wayside defect detection installations. Computer-Aided Civil and Infrastructure Engineering, 24 (5), 309{319(11).

Rajagopal, R., Varaiya, P., 2007. Health of californias loop detector system. California PATH Research Report,UCB-ITS-PRR-2007-13.

Sheffi, Y., 1985. Urban Transportation Networks: Equilibrium Analysis with Mathematical Programming Methods. Prentice-Hall, Inc., Englewood Cliffs, N.J.

Snyder, L. V., Daskin, M. S., 2005. Reliability models for facility location: The expected failure cost case. Transportation Sciense 39 (3), 400-416.

Yang, H., Iida, Y., Sasaki, T., 1991. An analysis of the reliability of an origin-destination trip matrix estimated from traffic counts. Transportation Research Part B 25 (5), 351-363.

Yang, H., Yang, C., Gan, L., 2006. Models and algorithms for the screen line-based traffic-counting location problems. Computers & Operations Research 33 (3), 836-858.

Yang, H., Zhou, J., 1998. Optimal traffic counting locations for origin-destination matrix estimation. Transportation Research Part B 32 (2), 109-126.